Mechanobiology in Medicine 2 (2024) 100095

Contents lists available at ScienceDirect

Mechanobiology in Medicine

journal homepage: www.sciencedirect.com/journal/mechanobiology-in-medicine

Full Length Article

Low-magnitude high-frequency vibration reduces prostate cancer growth and extravasation *in vitro*☆

Amel Sassi [a], Kimberly Seaman [b], Xin Song [b], Chun-Yu Lin [a], Yu Sun [a,b], Lidan You [a,b,c,*]

[a] Institute of Biomedical Engineering, University of Toronto, M5S 3G9, Canada
[b] Department of Mechanical & Industrial Engineering, University of Toronto, M5S 3G9, Canada
[c] Department of Mechanical and Materials Engineering, Queen's University, K7L 3N6, Canada

ARTICLE INFO

Keywords:
Low-magnitude high-frequency vibration
Mechanical loading
Vibration
Prostate cancer
Bone metastasis
Osteocyte
Microfluidic
Spheroid

ABSTRACT

Prostate cancer (PCa) continues to rank among the most common malignancies in Europe and North America with significant mortality rates despite advancements in detection and treatment. Physical activity is often recommended to PCa patients due to its benefits in preventing disease recurrence and managing treatment-related side effects. However, physical activity may be challenging for elderly or bedridden patients. As such, vibration therapy has been proposed as a safe, effective, and easy to perform alternative treatment that may confer similar effects as physical exercise. Specifically, low-magnitude high frequency (LMHF) vibration has been shown to decrease breast cancer extravasation into the bone and reduce other types of cancer proliferation by impacting cell viability. Here, we investigated the effects of daily application of LMHF vibration (0.3 g, 60 Hz, 1 hour/day for 3 days) on prostate cancer growth and bone metastasis *in vitro*. Our findings suggest that LMHF vibration significantly reduces colony formation through a decrease in cell growth and proliferation. Moreover, using a 3D cell culture model, LMHF vibration significantly reduces PC3 spheroid size. Additionally, LMHF vibration reduces PCa cell extravasation into the bone microenvironment through the stimulation of osteocytes and subsequent osteocyte-endothelial cell cross talk. These findings highlight the potential of LMHF vibration for managing PCa growth and metastasis.

1. Introduction

Prostate cancer (PCa) is the most common non-cutaneous cancers across Europe and North America, and it is expected that 1 in 8 men will be diagnosed during his lifetime.[1] According to the most recent published data, in 2023, there was 288,300 new cases of prostate cancer and 34,700 deaths from the disease in the United States.[2] Since 1993, the mortality rate of prostate cancer has been steadily declining, largely in part due to improved disease detection and treatment through surgery and radiation.[3] Despite the overall decline in mortality, PCa continues to rank third as the leading cause of cancer-related deaths, after lung and colorectal cancer.[3]

To improve survival, patients are often advised to make changes to their lifestyle. For many, this entails incorporating physical activity into their daily routine to either prevent disease recurrence, improve survival following diagnosis or to reduce the side effects of traditional treatments such as chemotherapy.[4,5] Notably, greater levels of physical activity are associated with reduced incidence of various cancers including PCa.[6–8] Physical activity directly and indirectly impacts biological pathways that influence the tumorigenic properties of PCa. Namely, direct mechanisms are attributed to myokines secreted by skeletal muscles which confer beneficial effects to metabolism through a reduction in insulin resistance, reduced adiposity, and enhanced glucose uptake.[9] Additionally, myokines such as IL-6, IL-15 and IL-10 inhibit cancer cell proliferation, promote apoptosis, and induce cell-cycle arrest.[9] Indirect mechanisms include a reduction in inflammation, improved immune function, a decrease in adiposity and overall enhancements in cardiorespiratory functions.[10,11] While most theories suggest interactions between global effects of exercise and PCa, the effects of the direct application of mechanical loading on cancer cells have garnered great attention.[12,13]

☆ Given her role as an Editor of this journal, Lidan You had no involvement in the peer-review of this article and has no access to information regarding its peer-review. Full responsibility for the peer-review process for this article was delegated to Da Jing.

* Corresponding author. Department of Mechanical and Materials Engineering, Queen's University, K7L 3N6, Canada.
E-mail addresses: amel.sassi@mail.utoronto.ca (A. Sassi), kimberly.seaman@utoronto.ca (K. Seaman), suzie.song@mail.utoronto.ca (X. Song), delphine.lin@mail.utoronto.ca (C.-Y. Lin), yu.sun@utoronto.ca (Y. Sun), you.lidan@queensu.ca (L. You).

https://doi.org/10.1016/j.mbm.2024.100095
Received 3 May 2024; Received in revised form 30 July 2024; Accepted 17 August 2024
Available online 26 August 2024

Different cell types within the body are subjected to diverse mechanical forces that modulate cellular machinery during development and homeostasis. Cells can convert physical stimuli to internal biochemical responses through mechanotransduction. Muscle cells were found to respond to mechanical stretch by triggering pathways to differentiate precursor cells.[14] Endothelial cells were reliant on shear forces generated by blood flow to regulate their gene expression profile.[15] Osteocytes in the bone sense mechanical stress and respond by signalling to surrounding osteoblasts and osteoclasts to regulate remodelling.[16]

Cancer cells, much like other mechanosensing cells are also able to detect and respond to mechanical forces which influence tumor progression and metastasis. Mechanical forces can arise from the stiffness of the extracellular matrix and from mechanical loading regimens such as tension, compression, shear forces and vibration. Notably, within the tumor microenvironment, cancer cells deposit aberrant extracellular matrix that influences tumor stiffness.[17] Cancer cells within the tumor are less stiff and more compliant than healthy cells, which promotes their migratory potential to distant metastatic sites through alterations in the cytoskeleton.[18] Additionally, mechanical loading to cancer cells has been shown to impact invasion, adhesion, viability, and cell metabolism. Depending on the type, duration and magnitude of the mechanical loading, cancer cells have been shown to exhibit varied effects. Mechanical stretch increases invadopodia and increases transmigration of cancerous cells.[19,20] Cancer cells exposed to fluid shear exhibit increased motility, metastatic potential, epithelial-mesenchymal transition and increased chemoresistance.[21–23] However, vibration has been shown to exert promising effects on tumor cell progression. Specifically, Yi et al. (2020), reported that low magnitude high frequency (<1 g, >30 Hz) vibration reduced the metastatic potential of breast cancer cells whereby the nucleus served as a critical mechanosensory organ to connect to the cytoskeleton and initiate mechanotransduction.[24] In contrast, Olcum et al. (2014) observed no significant differences in breast cancer invasion following treatment with low magnitude mechanical stimulus but reported a significant reduction in the number and viability of MDA-MB-231 cells through enhanced G1 and G2 arrest.[25] Moreover, a study conducted by Xiong et al. (2024) demonstrated that low intensity vibration applied directly to osteosarcoma cells altered their morphology and resulted in a decrease in cell viability and motility.[26]

Understanding the influence of mechanical forces on cancer cells is particularly crucial in the context of bone metastasis, a common complication of advanced PCa. Specifically, the bone serves as an active organ with the ability to remodel and adapt in response to loading, damage, and hormonal changes, with the goal of maintaining tissue integrity. Circulating tumor cells can attach to the endothelial cells of blood vessels and invade through the vessel wall into the marrow.[27,28] Once inside the bone, prostate cancer cells increase bone production by forming bone masses composed of loosely packed, randomly oriented collagen bundles of suboptimal strength.[3] Osteoclast activity also increases, suggesting that prostate cancer cells induce bone production through an overall increase in bone remodelling.[29,30] Therefore, metastatic cancer drastically disrupts bone homeostasis such that bone resorption and formation become unbalanced, resulting in osteolytic or osteoblastic bone lesions.[31] In the case of prostate cancer, bone metastases promote both forms of lesions through the production of pro-osteoblastic factors that promote bone mineralization and pro-osteoclastogenic factors that trigger the development and activity of osteoclasts.[32]

Mechanical loading due to physical activity is critical in maintaining homeostatic bone remodelling processes and the integrity of the bone.[33] During periods of physical activity, mechanical forces, sensed by osteocytes, cause the bone to switch from osteoclastic bone resorption to osteoblastic bone formation, resulting in an increase in bone mass.[33] In the absence of mechanical loading, bone resorption dominates, resulting in net bone loss.[33] Osteocytes, the most abundant cell type within the bone, accounts for approximately 90–95% of the total bone cell population, and exhibit mechanosensing abilities. Notably, osteocytes form a connected network, within the lacunar-canalicular system, through cellular processes known as dendrites that allow for rapid detection in changes in mechanical loading and downstream signal transductions. Consequently, given the role of osteocytes in regulating bone remodelling, and the fact that prostate cancer cells disrupt bone remodelling, osteocytes may be involved in regulating the process of bone metastasis.

As such, LMHF vibration has recently emerged as a safe, effective, and easy to perform adjuvant therapy that may induce similar effects as physical activity but is suitable for non-weight bearing patients. Specifically, LMHF vibration has been shown to activate osteocytes and reduce breast cancer bone extravasation.[34,35] The observed effects may be advantageous for elderly or bedridden patients, where physical activity may be challenging due to mobility impairments which put them at greater risk for fractures.[34,35] However, to date, this is the first study to examine the effects of LMHF vibration on prostate cancer growth or bone metastasis.

In this study, to address the gap in our understanding of how mechanical forces affect prostate cancer, we examined whether the direct application LMHF vibration impacts the tumorigenic properties of prostate cancer. Specifically, we examined the colony formation, cell growth, proliferation, apoptosis, and live/dead ratios using traditional 2D culture systems and examined changes in PC3 spheroid size using a 3D cell culture model. Additionally, we employed a bone metastasis-on-a-chip platform to investigate the effects of LMHF vibration on PCa extravasation.

2. Materials and methods

2.1. Cell culture

2.1.1. PC3

PC3 cells, a human prostate cancer cell line, (ATCC, Manassas, VA, USA) were cultured in Kaighn's Modification of Ham's F-12 Media (2127022; Gibco, USA), supplemented with 10% fetal bovine serum (FBS; 12483-020; Gibco, USA) and 1% penicillin streptomycin (15140122; P/S; Gibco, USA).

2.1.2. MLO-Y4

MLO-Y4 cells, a murine osteocyte-like cell line (a gift from Dr. Linda Bonewald, Indiana University, Indianapolis, IN, USA), were used as an osteocyte model. Cells were grown on cell culture dishes coated with 0.15 mg/mL type-I rat tail collagen (354236; Corning, USA) in 94% α-MEM basal media (12571063; Wisent, Canada), supplemented with 2.5% FBS, 2.5% calf serum (16010-159; Gibco, USA) and 1% P/S.

2.1.3. Human umbilical vein endothelial cells (HUVEC)

HUVECs (a gift from Dr. Craig Simmons, University of Toronto, Toronto, ON, Canada) were cultured in EndoMax basal media (301-010-CL; Wisent, Canada) supplemented with 2% EndoMax growth supplement (301-013-XL; Wisent, Canada), 10% FBS, and 1% P/S.

2.2. LMHF vibration platform

The custom-made vibration platform used throughout this study is shown in Fig. 1. Briefly, the platform allows for LMHF vibration to be generated and delivered to cells in a vertical and sinusoidal motion at magnitudes of 0.1–0.3 g amplitudes (1 g = 9.81 m/s^2) and frequencies of 30–90 Hz. The vibration platform utilizes a piezo-electric actuator (TDK Electronic AG, Germany) capable of reaching a maximum displacement of 230 μm to induce acceleration by moving the platform at a fixed displacement in a single direction. The Arduino Uno is connected to a Serial Peripheral Interface Analog-to-Digital converter to ensure consistent sinusoidal wave output. The magnitude of vibration was monitored using the output from the Analog-to-Digital converter in the Arduino

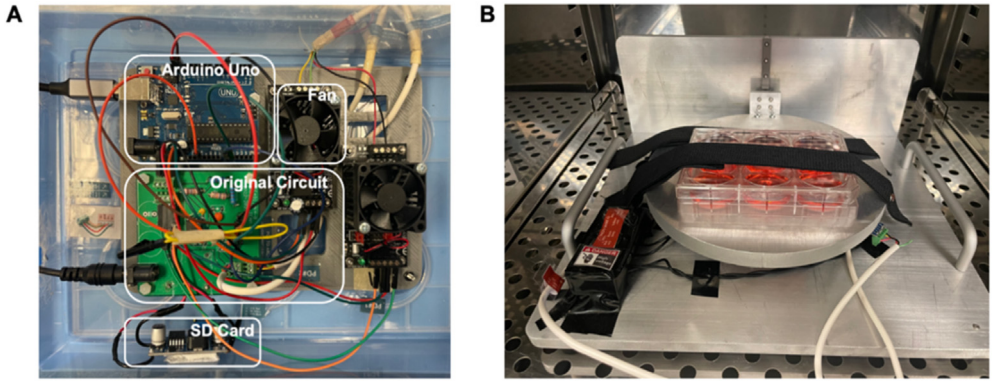

Fig. 1. **(A)** Circuitry of the vibration platform including a microcontroller (Arduino Uno), circuit board and SD card. **(B)** Vibration platform placed in the incubator with 6-well plate placed on top and strapped in place.

Uno. For all experiments, LMHF vibration was set to 0.3 g, 60 Hz for 1 hour due to its effects at reducing osteoclastogenesis[36] and at decreasing breast cancer extravasation.[34] Moreover, one key feature of the vibration platform is its ability to be placed in the incubator, allowing cells to remain under standard cell culture conditions to ensure that any changes are due to the effects of vibration rather than due to changes in atmospheric conditions or temperatures. Moreover, to ensure consistency in cell response to vibration, the volume of media in each well and each experiment was consistently used across all replicates.

2.3. Colony formation

PC3 cells were seeded in 6-well plates at a density of 1000 cells/well. Following incubation for 24 h in 5% CO_2 and 37 °C, cells were either treated with LMHF vibration for 3 consecutive days or remained under static conditions. Following treatment, growth media was replaced every 2 days. Cells were then fixed with 70% ethanol and stained with 0.5% Crystal Violet (CRY422,25; BioShop, Canada). Colonies (>50 cells) were counted manually, and percentage of area covered by colonies was quantified using the ImageJ plugin ColonyArea (NIH).

2.4. Cell growth

PC3 cells were seeded in 6-well plates at a density of 3.0×10^4 cells/well. Following incubation for 24 hours in 5% CO_2 and 37 °C, cells were either treated with LMHF vibration for 3 consecutive days or remained under static conditions. Media was renewed prior to each round of vibration. Growth curves were obtained by taking 5 random images in each well on each day and manually counting cells. Total cell count was determined by trypsinizing cells and counting the number of cells in 20 μL of solution using Trypan blue stain and a Haemocytometer.

2.5. MTT assay

PC3 cells were seeded in 96-well plates at a density of 2.0×10^3 cells/well. Following incubation for 24 hour in 5% CO_2 and 37 °C, cells were either treated with LMHF vibration for 3 consecutive days or remained under static conditions. Media was renewed prior to each round of vibration. Immediately following the final round of vibration, media was discarded by carefully aspirating the media and 50 μL of serum-free media and 50 μL of MTT Reagent (ab211091; Abcam, UK) was added into each well. Cells were incubated for 3 hours in 5% CO_2 and 37°C and sealed with Parafilm and covered with foil to prevent any interference with light. After incubation, 150 μL of MTT solvent was added into each well, and well plates were shaken on an orbital shaker for 15 min placed in the incubator. Absorbance was read at 590 nm using a Sunrise Microplate Reader (30214, TECAN, Switzerland).

2.6. Apoptosis

PC3 cells were seeded in 48-well plates at a density of 1.5×10^4 cells/well. Following incubation for 24 hours in 5% CO_2 and 37 °C, cells were either treated with LMHF vibration for 3 consecutive days or remained under static conditions. Apoptosis was assessed by staining cells with 5% APOPercentage™ dye (A1000; Biocolor; Carrickfergus, UK) for 30 min. 4 images were taken per well using a light microscope, as per the manufacturer's instructions, and the total number of cells and APOPercentage-stained cells were counted, and the percentage of apoptotic cells was calculated.

2.7. Live/dead staining

PC3 cells were seeded in 48-well plates at a density of 1.5×10^4 cells/well. Following incubation for 24 hours in 5% CO_2 and 37 °C, cells were either treated with LMHF vibration for 3 consecutive days or remained under static conditions. The number of live and dead cells was assessed by staining cells with 20 μL of NucGreen™ Dead (Dead cell indicator) (R37609; Thermo Fisher Scientific; Eugene, OR USA) and 20 μL of NucBlue™ Live (Total cell indicator) (R37609; Thermo Fisher Scientific; Eugene, OR USA) for 30 minutes. A negative control was established by treating cells with 70% ethanol for 15 min prior to staining. 4 images were taken per well using a fluorescence microscope (Nikon, Japan). The total number of cells and dead cells were counted, and the live/total cell ratio was calculated using ImageJ (NIH, Bethesda, MD, USA).

2.8. Spheroid production

PC3 cells were grown to 70% confluency and cell suspensions were prepared by washing cells with 7 mL of PBS and adding 3 mL of trypsin-EDTA solution for 4 minutes at 37 °C. Trypsin was neutralized with 2 mL of growth medium, and the suspension was centrifuged at 1150 g for 7 min. The cell pellet was resuspended, and the suspension was diluted with cold growth medium and Matrigel (354234; Corning USA) to dispense 15,000 cells into 96-well ultra-low attachment plates (7007; Corning, USA). Spheroid diameter was calculated by imaging spheroids on each day using a standard brightfield microscope and measuring the area of the 2D images using ImageJ and converted to diameter assuming a spherical shape.

2.9. Microfluidic platform fabrication

The bone-metastasis-on-a-chip model was fabricated by following standard photolithography procedures using the design outlined in Mei et al. (2019).[37] Using both SU-8 2050 (Y111072; Microchem, USA) and 2075 (Y111074; Microchem, USA), designs of the osteocyte, lumen and side channels photomasks were imprinted using UV exposure from a EVG

620 Mask Aligner on the spin-coated silicon wafer. Following fabrication of the master, the microfluidic device was fabricated with poly-dimethyl-siloxane (PDMS) and curing agent (04019862; Dow Chemical, USA) at a 10:1 ratio. The device was cut, and inlet and outlets were generated with biopsy punches, and plasma bonded to a 75 mm × 50 mm microslide after 90-s oxygen plasma treatment.

2.10. Microchannel environment

The osteocyte channel was coated with 0.15 mg/mL type-1 rat-tail collagen for 1 hour. The microchannels were coated with 100 μg/mL fibronectin solution (F1141-2 MG; Sigma–Aldrich, USA) for 40 minutes at 4 °C. The lumen channel was coated with a hydrogel solution with 11.07 mg/mL type-1 rat-tail collagen (354249; Corning, USA) and 7.6 mg/mL of Matrigel (CACB354230; Corning, USA) and was slowly removed after 30 seconds to form the lumen. The devices were then incubated in a water bath for 1 hour before adding the respective media into each channel.

2.11. Microchannel validation

To validate whether endothelial cells could both survive and maintain the appropriate junctions to serve as a physiological barrier for cancer extravasation throughout the experiment, HUVECs were seeded into the hydrogel lumen at 2.0×10^6 cells/mL on all sides. Microfluidic devices were placed in the incubator at 5% CO_2 and 37 °C and media was replaced every 24 hours for 96 hours. HUVECs were then fixed with 10% formalin (HT501128; Sigma–Aldrich, USA), and stained with DAPI and VE-cadherin primary antibody (AF938-SP; Abcam, UK) and secondary antibody conjugated to AlexaFluor™ 488 (donkey anti-goat IgG (H+L); Thermofisher, USA). Cells were then imaged using a Confocal Microscope (Leica, Germany) (Supplementary Fig. 1).

2.12. Prostate cancer cell extravasation

Cells were seeded based on the procedures outlined in Mei et al. (2019).[37] Briefly, HUVECs were seeded at 2.0×10^6 cells/mL to the bottom and side of the device to form the lumen channel. MLO-Y4 cells were seeded into the osteocyte channel at a density of 1.5×10^6 cells/mL. Cells were left to attach for 3 hours prior to seeding PC3 cells fluorescently labelled with CellTracker™ Green (C2925; Invitrogen, USA) at 4.0×10^6 cells/mL. Prostate cancer cells were seeded to the bottom and side of the device. After confirming successful attachment of cells after 24 hours, microfluidic devices with the respective cells were placed on the custom-made vibration platform for 1 hour every day for 3 consecutive days. Extravasation distance was calculated by comparing distance travelled in the side channel using fluorescent images on day 1 and day 4 (Supplementary Fig. 2).

2.13. Effects of LMHF vibration on prostate cancer cell extravasation without osteocytes

To confirm whether LMHF vibration directly stimulates PC3 cells to reduce extravasation, only HUVECs and PC3s were seeded into the microfluidic platform. HUVECs were seeded at 2.0×10^6 cells/mL to the bottom and side of the device to form the lumen channel. Cells were left to attach for 3 hours prior to seeding PC3 cells fluorescently labelled with CellTracker™ Green at 4.0×10^6 cells/mL. Prostate cancer cells were seeded to the bottom and side of the device. Microfluidic devices with the respective cells were placed on the custom-made vibration platform for 1 hour every day for 3 consecutive days. Extravasation distance was calculated by comparing distance travelled in the side channel using fluorescent images on day 1 and day 4 (Supplementary Fig. 2).

2.14. Conditioned media collection

MLO-Y4 cells were cultured on collagen coated 6 well plates until cells reached 80% confluency. Cells were then vibrated at 0.3 g and 60 Hz for 1 hour. Media was replaced prior to vibrating cells. Conditioned medium (CM) containing soluble factors from vibration stimulated MLO-Y4 cells was collected following a 3-hour incubation. Additionally, static CM was collected from MLO-Y4 cells left undisturbed.

2.15. Adhesion to the endothelial monolayer

μ-Slide VI 0.4 (ibidi, Martinsried, Bavaria, Germany) were collagen coated with 0.15 mg/mL type-I rat tail collagen (354236; Corning, USA) for 1 hour at room temperature. HUVECs were seeded at 5.0×10^5 cells/mL. Once confluent, HUVECs were treated with static or vibration-stimulated MLO-Y4 CM for 16 hours. PC3 cells stained with CellTracker™ Green were then added to the treated HUVEC-coated channels at 800,000 cells/mL and were placed in the incubator for 30 minutes. Paired channels were rinsed gently three times with PC3 media, and the order within each pair was randomized to avoid any time-dependent variations. Channels were then imaged using a fluorescence microscope. The number of adhered cells were counted using ImageJ. Blocking experiments were performed in a similar manner. However, 1 ug/mL anti-human VCAM-1 neutralizing antibody was added to MLO-Y4 CM and used to treat HUVECs for 1.5 hours prior to the addition of fluorescently labelled PC3 cells. To carry out VCAM-1 immunostaining, HUVECs were seeded, grown and treated with MLO-Y4 CM as described above. However, following treatment for 16 hours, cells were fixed for 10 minutes, permeabilized with 0.3% Triton-X for 5 minutes and blocking buffer was added for 1 hour. The primary antibody solution (hVCAM-1, BBA10, Cedarlane, CA) was added and the microchannels were placed in the 4 °C fridge overnight. The secondary antibody solution (AlexaFluor™ 488) was added the following day for 2 hours at room temperature. The cells were then counterstained with DAPI and imaged using a fluorescent microscope. Mean intensity of VCAM-1 was quantified by quantifying the fluorescence of 10 random cells using ImageJ in each of the 10 randomly captured images of each of the microchannels.

2.16. Statistics

To detect statistical significance between static and vibration conditions, student *t*-tests (two-tailed) were performed. To examine effects of vibration across multiple days for cell growth or spheroid diameter, a two-way analysis of variance (ANOVA) was carried out followed by a two-stage step-up method of Benjamini, Krieger and Yekutieli correction to control for false discovery rate. GraphPad Prism software version 9.5.1 (GraphPad Software Inc., San Diego, CA, USA) was used to complete all statistical analyses. Results with p-values less than or equal to 0.05 were considered statistically significant ($^*P \leq 0.05$, $^{**}P \leq 0.01$, $^{***}P \leq 0.001$, $^{****}P \leq 0.0001$). All experiments were replicated at least three times, using a fresh vial of cells for each experiment, with at least six technical replicates. Each replicate was determined to be statistically significant.

3. Results

3.1. LMHF vibration significantly reduces PC3 colony formation

To determine effects of LMHF vibration on the reproductive cell survival of PC3 cells, a clonogenic assay was carried out. A significant decrease in the total number of colonies (Fig. 2A) and percent area covered by colonies (Fig. 2B) was observed in PC3s exposed to LMHF vibration when compared to static conditions (Fig. 2C). To investigate whether the observed reduction in cell growth and colony formation was due to an increase in cell detachment from the well plates, we examined the total number of detached cells

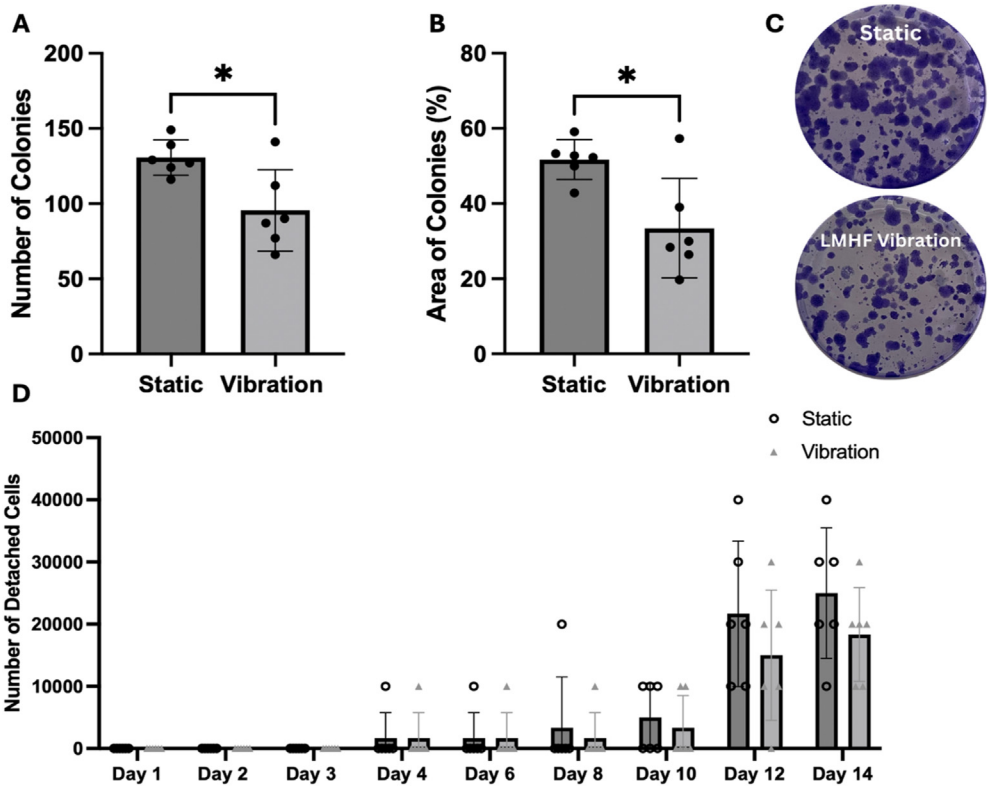

Fig. 2. (A) Number of colonies and **(B)** percent area covered by colonies of prostate cancer cells under static and LMHF vibration conditions (0.3 g, 60 Hz, 1 h/day for 3 days), n = 6 wells. **(C)** Representative images of wells containing Crystal Violet stained PC3 cells under static or LMHF vibration conditions. **(D)** Total number of PC3 cells in static or vibration conditions detached from cell culture plate when carrying out colony formation assay, n = 6 wells. Cells were counted by staining cells with Trypan Blue and counting cells using a Haemocytometer. Data are represented as mean ± standard deviation $*p < 0.05$.

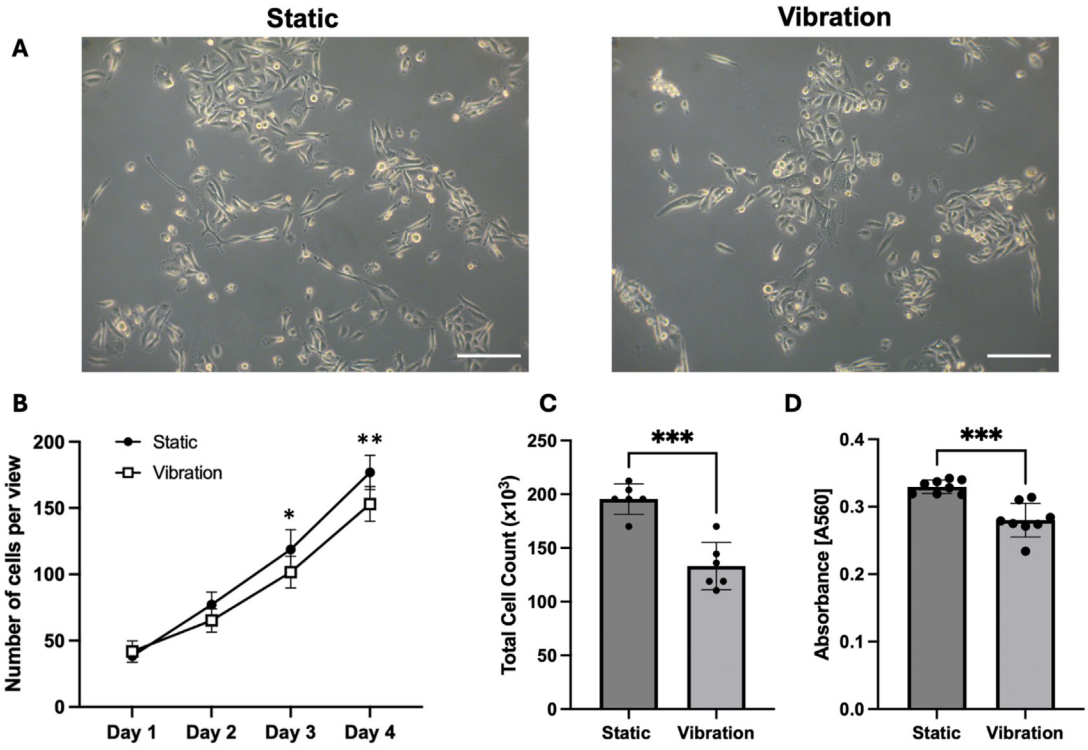

Fig. 3. (A) Microscopic images of PC3 cells with and without treatment with LMHF vibration (0.3 g, 60 Hz, 1 h/day for 3 days). Images were taken using a light microscope at a total magnification of 20x. **(B)** Cell growth curves for PC3 cells under static and vibration conditions. Number of cells per view was determined by manually counting cells from 5 random microscopic images taken per well and taking the average of all 5 images, n = 6 wells. **(C)** Total number of PC3 cells in static or vibration conditions, n = 6 wells. Cells were counted by staining cells with Trypan Blue and counting cells using a Haemocytometer. **(D)** Cell proliferation of PC3 cells treated with and without LMHF vibration quantified using an MTT assay, n = 8 wells. Data are represented as mean ± standard deviation. $*p < 0.05$, $**p < 0.01$, $***p < 0.001$. Scale bar = 100 μm.

in the media every time the media was changed. Specifically, 20 μL of media was removed and diluted with Trypan Blue stain. PC3 cells that detached from the cell culture plate were counted using a Haemocytometer. No significant differences in the number of detached cells were observed between static and vibration treated PC3s (Fig. 2D). Moreover, during the treatment period (day 1-day 4), little to no cells were found in the media.

3.2. LMHF vibration significantly reduces PC3 cell growth

Additionally, the direct application of LMHF vibration significantly reduced the number of cells on day 3 and day 4 (Fig. 3). When comparing growth between day 1 and day 4, PC3 cells that remained static experienced a 361% increase in the total number of cells while cells that were treated with LMHF vibration had a 266% increase. No significant differences in cell count were observed between the two groups in the absence of treatment (day 1) and after one round of vibration (day 2). However, for the static group, the percent increase in cell growth from day 1 to day 2 for cells under static conditions was determined to be 101% and 56% for cells treated with one round of LMHF vibration. The difference in total cell count between the two conditions was also determined to further validate the cell growth findings. A significant decrease in the number of PC3 cells was discovered following treatment with LMHF vibration (Fig. 3C) Moreover, while no distinct changes in cell morphology were observed, PC3 cells treated with vibration displayed a subtle rounder appearance compared to those that remained static (Fig. 3A). We further assessed the effects of LMHF vibration on PC3 proliferation using an MTT assay. Following 3 bouts of vibration, a significant decrease in MTT-based cell proliferation was observed (Fig. 3D).

3.3. LMHF vibration does not significantly affect PC3 viability or apoptosis

To investigate whether the observed reduction in cell growth was due to increased cell death, an apoptosis and live/dead assay was carried out. No significant differences in the percentage of apoptotic (Fig. 4A and B) or percentage of live/total (Fig. 4C and D) PC3 cells were discovered between LMHF vibration and the control group.

3.4. LMHF vibration significantly reduces PC3 spheroid diameter

Given the limitations of two-dimensional monolayers to recapitulate the normal tumor cell environment, we further examined how LMHF vibration impacts PC3 tumor cell growth in a three-dimensional culture. Specifically, spheroids have been shown to mimic the mechanical forces present in the tumor which provides a more physiologically relevant model. Our results indicate that PC3 spheroid diameter significantly decreases on day 2, 3 and 4 which is following 1, 2 and 3 rounds of vibration, respectively (Fig. 5B). Additionally, when comparing change in spheroid diameter on between day 1 and day 4, spheroids treated with LMHF vibration display significantly decreased values (Fig. 5C).

3.5. LMHF vibration stimulated osteocytes decrease prostate cancer extravasation

Due to the propensity of prostate cancer to metastasize to the bone, we investigated the effects of LMHF vibration on prostate cancer extravasation into the bone. Namely, we measured the extravasation distance of PC3 cells seeded into a bone metastasis-on-a-chip platform under static and LMHF vibration conditions. Briefly, the bone metastasis-on-a-chip platform is composed of a PDMS device plasma bonded to a 75 mm × 50 mm microslide (Fig. 6A) with two adjacent channels: the osteocyte channel and the lumen channel. The osteocyte microchannel is collagen-coated and contains MLO-Y4 cells seeded at a density of 1.5×10^6 cells/mL (Fig. 6B and C). The lumen channel is composed of HUVECs seeded at 2.0×10^6 cells/mL to the bottom and side of the device to mimic a blood vessel, with fluorescently labelled PC3 cells seeded at 4.0×10^6 cells/mL (Fig. 6B and C). Furthermore, our validation experiment

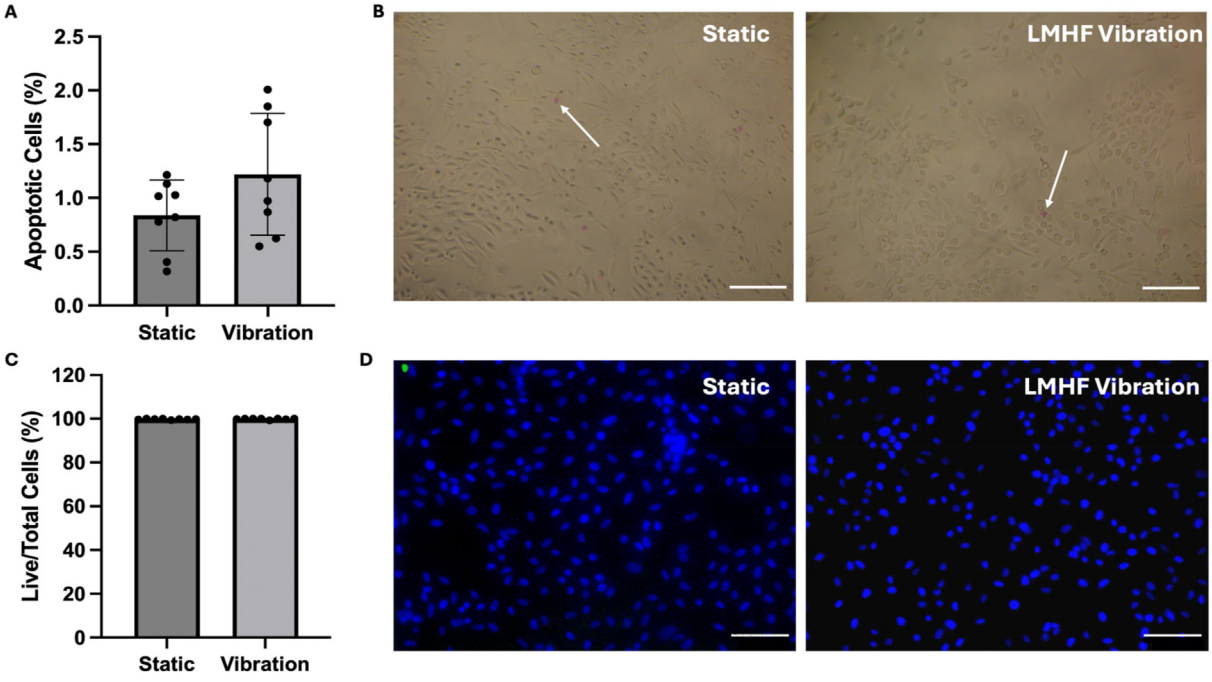

Fig. 4. Histograms displaying the percentage of **(A)** apoptotic and **(C)** live/total prostate cancer cells under static and LMHF vibration conditions (0.3 g, 60 Hz, 1 hour/day for 3 days) n = 8 wells. Representative microscopic images of (**B**) APOPercentage stained, pink, cells indicated with the white arrow and (**D**) live cells (blue) and dead cells (green) under static or vibration conditions, n = 8. Data are represented as mean ± standard deviation. Scale bar = 100 μm.

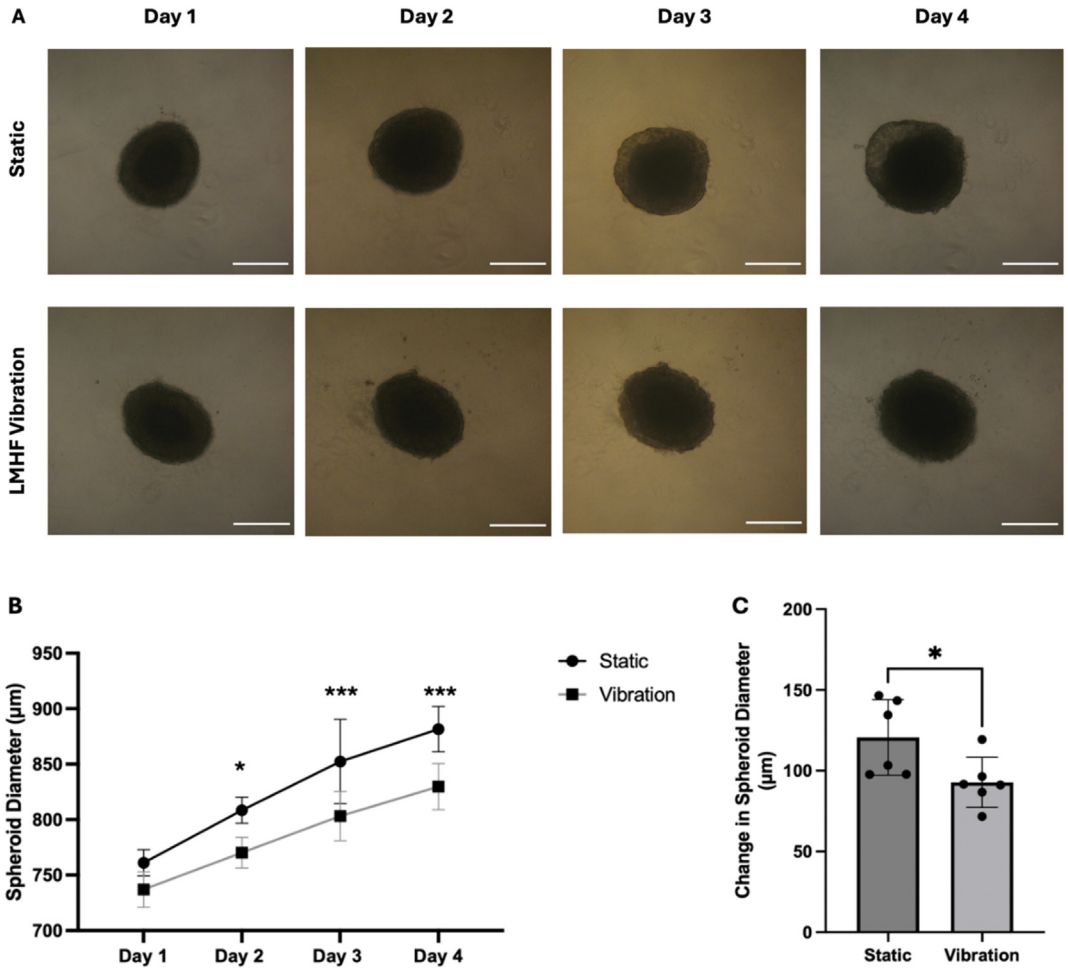

Fig. 5. **(A)** Representative images of PC3 spheroids under static or LMHF vibration (0.3 g, 60 Hz, 1 h/day for 3 days) conditions grown at a density of 15,000 cells between day 1 and day 4. **(B)** Plot of growth kinetics represented as spheroid diameter for PC3 spheroids under static or vibration conditions. **(C)** Change in spheroid diameter between day 4 and day 1 for PC3 cells treated with or without LMHF vibration. Data are represented as mean ± standard deviation, n = 6 spheroids. $^{*}p < 0.05$, $^{***}p < 0.001$. Scale bar = 500 μm.

demonstrated that the intercellular junctions of endothelial cells are maintained for the 96-h duration of our study (Supplementary Fig. 1).

Extravasation distance was calculated by comparing the distance travelled into the side channel using fluorescent images from day 1 and day 4 (Supplementary Fig. 2). We observed a significant reduction in PC3 cell extravasation distance (Fig. 7A, C) and the number of extravasated cells (Fig. 7B and C) in cells treated with LMHF vibration when compared to the static group. To explore whether the observed results were because of LMHF vibration on osteocytes or directly on PC3 cells, we examined the extravasation distance of prostate cancer cells in the absence of MLO-Y4s. Using the bone metastasis-on-a-chip model, only HUVEC endothelial cells and PC3 cells were seeded into the lumen channel. Following treatment with LMHF vibration for three days, there was no significant difference in extravasation distance (Fig. 7D, F) or the number of extravasated cells (Fig. 7E and F) observed between the two groups.

3.6. LMHF vibration-stimulated osteocytes reduce prostate cancer cell adhesion onto the endothelial monolayer

To investigate potential mechanisms involved in the observed reduction in PC3 extravasation following exposure to LMHF vibration, we examined whether soluble factors from vibration-stimulated osteocytes impacted prostate cancer cell adhesion to the endothelial monolayer. HUVECs were grown to confluency and treated with either static or vibration-stimulated MLO-Y4 conditioned media (CM) for 16 hours. Fluorescently labelled PC3 cells were seeded onto the HUVEC monolayer and incubated for 30 minutes before washing away loosely adhered cells. We observed a significant decrease in the number of PC3 cells that remained adhered to the HUVECs treated with CM from vibration-stimulated osteocytes when compared to HUVECs treated with static MLO-Y4 CM (Fig. 8A and B). Specifically, 29% more PC3 cells remained adhered to HUVECs treated with static MLO-Y4 CM when compared to vibration MLO-Y4 CM. Given previous findings that suggest that VCAM-1 is critical for prostate cancer cell adhesion to the endothelium and the initiation of extravasation, we investigated its potential role in the difference between treatment with static and vibration osteocyte CM. Since selectins may also influence the adhesion of PC3 cells onto the endothelium, a 16-hour incubation period was selected because their increased expression returns to basal levels after 6–12 hours.[38] Following incubation with the anti-VCAM-1 neutralizing antibody, the difference in static and vibration osteocyte CM groups was abolished (Fig. 8C and D). We further validated these results through an immunostaining experiment where we saw a reduction in VCAM-1 expression on endothelial cells treated with vibration-stimulated osteocyte CM (Fig. 8E). Fig. 8F highlights the visible reduction in the fluorescent VCAM-1 signals in cells treated with LMHF vibration-stimulated MLO-Y4 CM. That is, HUVECs treated with static CM show strong fluorescent signals on the outer periphery of the cell. Alternatively, HUVECs treated with vibration CM lack or have very low intensity signals.

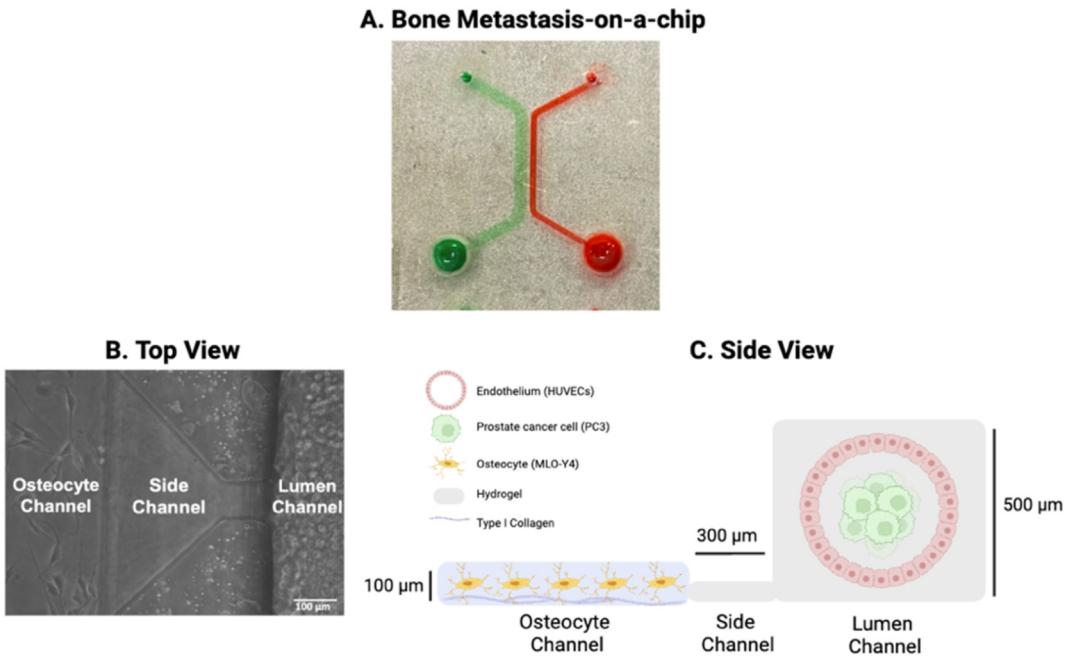

Fig. 6. Image displaying **(A)** PDMS device with lumen channel dyed red and osteocyte channel dyed green and **(B)** top microscopic view of microchannels and **(C)** cellular constituents and dimensions.

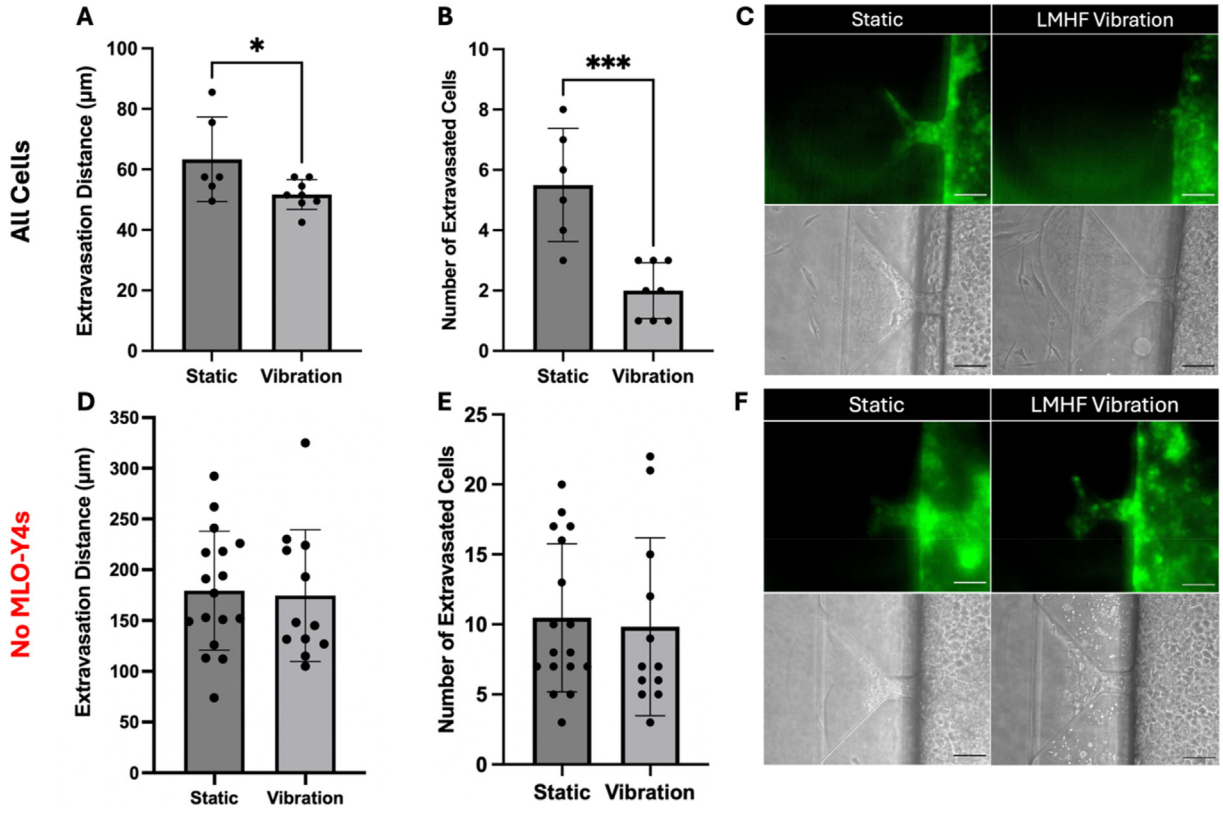

Fig. 7. Histograms comparing **(A)** PC3 extravasation distance (µm) and **(B)** the total number of extravasated cells under static (n = 6 channels) and LMHF vibration (0.3 g, 60 Hz, 1 h/day for 3 days, n = 8). **(C)** Fluorescent and brightfield microscopic images of PC3 cancer cell extravasation. Histograms comparing **(D)** PC3 extravasation distance (µm) **(E)** the total number of extravasated cells under static (n = 17) and LMHF vibration (0.3 g, 60 Hz, 1 h/day for 3 days, n = 12) in the absence of MLO-Y4s. Data are represented as mean ± standard deviation, $*p < 0.05$, $***p < 0.001$ **(F)** Fluorescent and brightfield microscopic images of PC3 cancer cell extravasation in the absence of osteocytes. Scale bar = 100 µm.

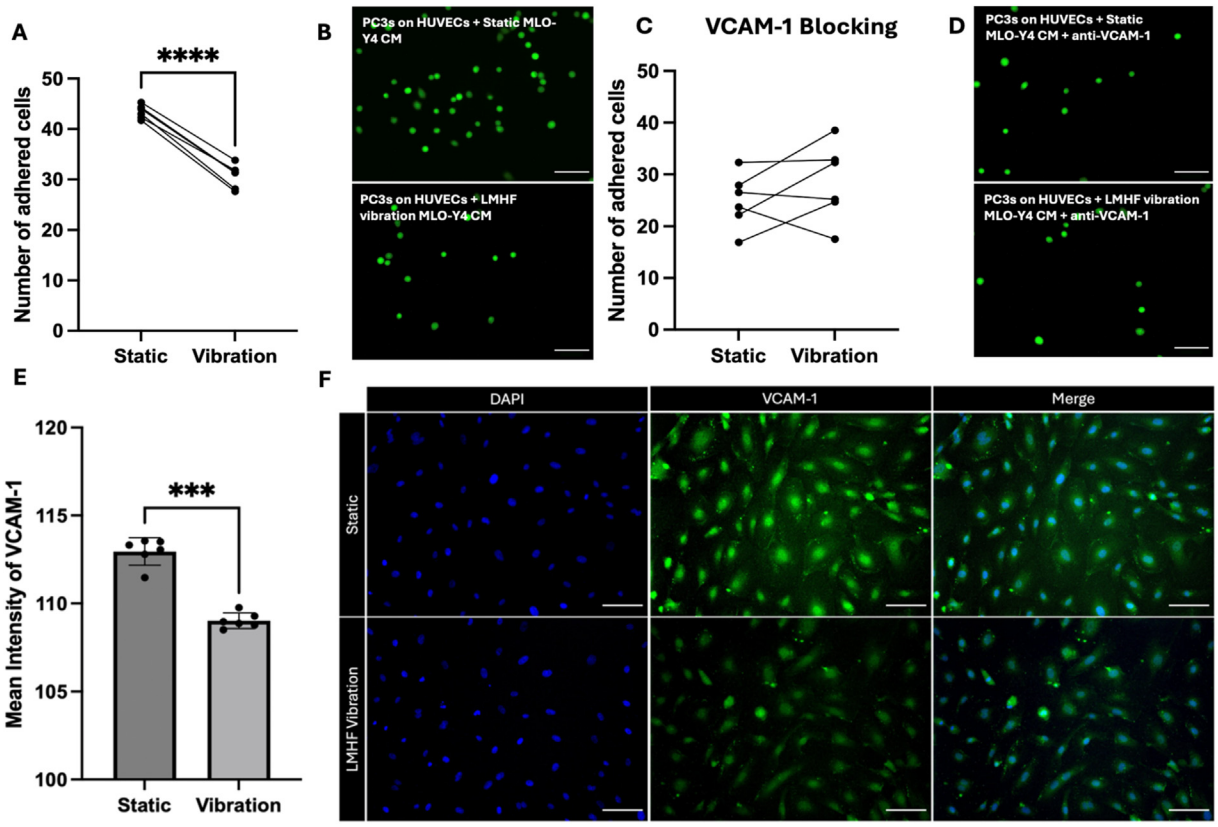

Fig. 8. **(A)** PC3 adhesion to endothelial monolayer in static or LMHF vibration osteocyte condition media, n = 6 microchannels. **(B)** Fluorescent images of PC3 cells on endothelial monolayers treated with static or LMHF vibration-stimulated MLO-Y4 CM. **(C)** Prostate cancer cell adhesion to the endothelial monolayer conditioned in osteocyte CM with anti-VCAM-1 neutralizing antibody, n = 6 microchannels. **(D)** Fluorescent images of PC3 cells on endothelial monolayers treated with static or LMHF vibration-stimulated MLO-Y4 CM and anti-VCAM-1 antibody. **(E)** Histogram and **(F)** representative fluorescent images of DAPI (blue) and VCAM-1 (green) comparing mean intensity in VCAM-1 expression in HUVECs treated with static or vibration-stimulated MLO-Y4 CM, n = 6 microchannels. Data are presented as paired data between static and vibration groups, ***$p < 0.001$, ****$p < 0.0001$. Scale bar = 100 μm.

4. Discussion

In this study, we investigated the effects of LMHF vibration (0.3 g, 60 Hz for 1 h, for 3 days) on PC3 colony formation, cell growth, proliferation, apoptosis, and live/dead ratios using a standard 2D cell culture system. We further validated our findings by examining the effects of LMHF vibration on PC3 spheroid size. Furthermore, we determined the effects of vibration-stimulated osteocytes on PC3 extravasation using a bone metastasis-on-a-chip platform. Our results indicated that LMHF vibration significantly reduces PC3 colony formation (Fig. 2), cell growth (Fig. 3B) and total cell count (Fig. 3C). Nevertheless, the observed reduction was likely due to the effects of LMHF vibration on cancer cell proliferation (Fig. 3D) as no changes in apoptosis (Fig. 4A) or the percentage of live cells (Fig. 4C) were observed. These results mirrored our findings using the 3D cell culture model as a significant reduction in PC3 spheroid diameter and therefore volume was determined (Fig. 5). Moreover, using our bone metastasis-on-a-chip platform (Fig. 6), we reported a reduction in prostate cancer cell extravasation distance and the number of extravasated cells (Fig. 7A–C). However, in the absence of osteocytes, no changes between static and vibration groups were reported (Fig. 7D–F). When examining specific mechanisms, our data suggests that vibration-stimulated osteocytes secrete soluble factors that indirectly affect PC3 extravasation through a reduction in adhesion of PC3 cells to endothelial cells through due to a decrease in VCAM-1 expression (Fig. 8).

The mechanistic insights into the effects of low-magnitude high-frequency vibration on cancer cells offer promising avenues for therapeutic interventions. Previous *in vitro* studies have been carried out to investigate the effects of vibration on other types of cancer cells such as breast cancer and osteosarcoma[25,26] but not on prostate cancer. Specifically, Olcum et al. (2014) reported a significant reduction in the number and proliferation of MDA-MB 231 cells following treatment of cells with 0.15 g and 90 Hz for 15 minutes/day, 5 days per week for 19 days.[25] Whereby vibration reduced the number of proliferating cells by arresting them in the G1 or G2 phase of the cell cycle. Our findings further support the anti-proliferative effects of vibration on prostate cancer cells. That is, in this study, we showed that the direct application of LMHF vibration on PC3 cells inhibited their cell growth and total cell count following 3 days of treatment (Fig. 3B and C). Conversely, Olcum et al. (2014) reported that the total number of cells was only significantly reduced on day 9. However, a slight non-significant reduction in the total number of cells on day 5 was observed. Interestingly, the *proliferation* of MDA-MB 231 cells was significantly decreased from day 5 onwards. Furthermore, while our current study does not examine the number of cells in each phase of the cell cycle, the significant reduction in cell growth and colony formation of PC3 cells as well as a significant reduction in proliferation measured through the MTT assay provide evidence for a decrease in cancer cell proliferation. Future flow cytometry analyses would provide valuable insights into the precise mechanism of the effects on the cell cycle.

Another key finding reported by Olcum et al. (2014) was the absence of effects on non-cancerous control cells. Our lab has previously characterized the effects of LMHF vibration on both viability and total cell count of MLO-Y4 cells and HUVECs [34; Fig. 2]. Similar to the results reported by Olcum et al. (2014), LMHF vibration had no effects on healthy cells.[25] These preliminary findings are particularly important for the clinical translation of LMHF vibration as an adjuvant therapy for patients with prostate cancer. Namely, in earlier clinical studies

examining the effects of whole-body vibration, no adverse effects were reported for all ages including children, adolescents,[39] adults,[40] or the elderly.[41,42] However, in a feasibility study, Oschwald et al. (2022) reported two cases of bleeding in patients with low platelet count following treatment with vibration over the course of three days.[39] When establishing a threshold for whole body vibration participation to 30,000 platelets/μL, no additional incidents of bleeding occurred. Since thrombocytopenia has an incidence rate of 12.3/100000 patient years this is unlikely to pose a concern for PCa patients in the clinical setting.[43,44]

Similarly, Xiong et al. (2024) investigated the effects of various frequencies of low intensity vibration on osteosarcoma cells. They observed that treatment with vibration (60 and 90 Hz frequencies, 0.3 g and 0.7 g magnitudes) for 20 minutes significantly altered the morphology of the examined cell lines through a reduction in surface contact area.[26] The osteosarcoma cell lines TT2 and U2OS also demonstrated a significant decrease in proliferation following treatment with vibration (0.3 g and 0.7 g, 90 Hz). The researchers also reported a significant reduction in cell motility in all osteosarcoma cell lines tested.[26] While no specific modal analyses were carried out, through observations alone, we noticed that vibration treated PC3 cells displayed a rounder morphology in comparison to static cells (Fig. 3A). The rounded morphology of PC3s may be an indicator of several changes including halted progression through the cell cycle,[45] as well as increased epithelial-mesenchymal transition.[46] Further comprehensive biomechanical downstream analyses are required to characterize the precise effects of LMHF vibration on PC3 cell morphology. Nevertheless, our reported changes in cell growth, colony formation and proliferation are further supported by the reduction in proliferation discovered by Xiong et al. (2024).[26]

As for *in vivo* research, additional animal studies have provided evidence that vibration could decrease the overall tumor burden. In a study carried out by Pagnotti et al. (2016), immunocompromised mice injected with human myeloma cells had a 31% lower tumor burden in the marrow following daily treatment with low intensity vibration (0.3 g, 90 Hz, 15 min per day for 8 weeks).[47] By the same token, Pagnotti et al. (2012) demonstrated that female mice prone to developing granulosa cell tumors that were treated with low intensity vibration (0.3 g, 90 Hz, 15 min per day for 1 year) exhibited a 30% decrease in tumor incidence.[48] To mimic the tumor microenvironment, we employed 3D spheroids to study how LMHF vibration could influence tumor growth in a system that already experiences mechanical forces through interacting cancer cells (Fig. 5). Our results using 3D spheroids provide additional evidence regarding the anti-proliferative effects of LMHF vibration using *in vitro* models. The convergence of our *in vitro* studies with these two *in vivo* models may further support the translational potential of LMHF vibration in the clinical setting.

While the precise mechanism of how LMHF vibration can impact cancer cell proliferation remains unknown, preliminary modal analyses by Xiong et al. (2024) provided concrete evidence that the efficacy of vibration is largely dependent on both cell rigidity and shape.[26] They estimated the intrinsic frequencies of cells with soft, intermediate, and rigid properties and discovered that the relationship between intrinsic frequency and Young's modulus is near linear. These findings suggest that cells that are less stiff can respond to external low intensity vibrations that resonate with their intrinsic frequencies. Specifically, the study highlighted that low intensity vibration had the ability to inhibit the progression of osteosarcoma through a reduction in cell viability but does not harm healthy cells. Rather low intensity vibrations promoted the conversion of mesenchymal stem cells (MSCs) into induced tumor-suppressing cells.

Targeting cancer cells based on biophysical properties such their resonant frequencies has been proposed and explored by other researchers. Namely, cancer cells have consistently been shown to be softer than healthy cells allowing them to be targeted using lower frequencies.[49,50] As such, previous studies have attempted to selectively target cancer cells using ultrasound harmonic excitation,[51] as well as radiofrequency electromagnetic fields[52] to enhance cellular oscillations and induce harmonic resonance to negatively affect cancer cell growth. The findings by Xiong et al. (2024) suggest a similar mechanism whereby low intensity vertical vibrations (0.3 g – 1 g, 30–90 Hz) are applied directly onto the cancer cells and induce cell death when cancer cells absorb the energy at the resonant frequency (30–90 Hz). Alternatively, healthy MSCs absorb minimal energy, due to their higher intrinsic frequencies. Therefore, the vibration serves as a mechanical stimulus to activate pathways that lead to the expression of tumor suppressor proteins such as procollagen C endopeptidase enhancer, aldolase A, histone H4, and peptidylpropyl isomerase B instead. Yet additional work into the precise mechanism and effects on how cells respond to such mechanical stimuli must be explored to fully understand the mechanism.

In addition, a pivotal aspect of our investigation focused on the effects of LMHF vibration on prostate cancer extravasation into the bone, a crucial step in the establishment of bone metastases. Our findings indicate a 37% reduction in the extravasation distance, and a 45% decrease in the total number of extravasated PC3 cells in our bone-metastasis-on-a-chip platform under LMHF vibration conditions (Fig. 7). Importantly, no significant reduction was observed when prostate cancer cells were seeded in the absence of osteocytes, highlighting the role of osteocytes in mediating the anti-metastatic effects of LMHF vibration. Notably, our study examines extravasation over the course of four days, which is consistent with previous work investigating early metastasis.[34]

It should be noted that osteocytes serve as the main mechanosensors that regulate bone remodelling in response to mechanical forces and represent over 90% of bone cells.[53] Upon the detection of changes in mechanical loading a variety of intracellular signalling pathways are activated. Remarkably, our lab previously reported that MLO-Y4 cells treated with LMHF vibration exhibited significant changes to various mechanosensitive genes following treatment [34; Fig. 2]. Specifically, a greater increase in Piezo1, COX-2 expression and a significant decrease in RANKL and RANKL/OPG expression was reported. Lau et al. (2010) reported similar results in gene expression changes, but also reported a significant decrease in prostaglandin E2 [36; Fig. 2]. These results suggest that MLO-Y4 cells can sense LMHF vibration and activate pathways involved in osteocyte mechanotransduction.

With regards to the effects of osteocyte mechanical stimulation and its regulation of cancer metastasis, existing literature is largely conflicting. Specifically, while some studies report that mechanical stimulation of osteocytes decreases invasion of cancer cells,[34,54,55] others report an increase in migration.[56,57] Our lab has previously shown, through conditioned media experiments, that stimulation of osteocytes with oscillatory fluid flow reduces the transendothelial migration of MDA-MB 231 breast cancer cells.[58] Additional experiments done by our lab using the microfluidic device shown in this study demonstrated a similar reduction in MDA-MB 231 breast cancer cell extravasation following treatment with low-magnitude high-frequency vibration.[34] Moreover, van Santen et al. (2023) demonstrated that DU145 prostate cancer cells treated with conditioned media from shear loaded human osteocyte-like cells exhibited a 1.34-fold decrease in invasion and no change in proliferation.[55] More specifically, the conditioned media enhanced the expression of epithelial genes SYND1 and CDH1, and it also enhanced mesenchymal genes VMN, Snail and MIP2.

In contrast, *in vitro* conditioned media studies carried out by Verbruggen et al. (2021) showed that soluble factors released by osteocytes inhibited breast and prostate cancer proliferation and invasion.[59] However, following mechanical stimulation with oscillatory fluid flow mechanical stimulation reversed such effects on breast cancer cells, and had no effect on prostate cancer cells. Using a microfluidic organ-on-a-chip model, they further demonstrated that mechanical stimulation of osteocytes results in increased invasion of breast and prostate cancer cells. However, several distinctions between our microfluidic devices exist. Firstly, the organ-on-a-chip platform utilized by Verbruggen et al. (2021) lacks the presence of endothelial cells, and the incorporation of hydrogel. Rather, their device is composed of a PDMS membrane with two collagen coated channels, which is a greater representation of the effects of

osteocyte mechanical stimulation in the presence of established bone metastases. Our research largely focuses on earlier stages of bone metastases during the process of extravasation, and how mechanical stimulation of osteocytes could be employed to reduce the overall tumor burden within the bone. As such, while results are conflicting, our data demonstrates that osteocytes play a critical role in the regulation of prostate cancer extravasation and mechanical stimulation through LMHF vibration may work to reduce extravasation.

Interestingly, we reported no significant difference in prostate cancer extravasation in the absence of osteocytes. Using the same microfluidic device, Song et al. (2022) discovered similar findings in breast cancer cells.[34] However, other studies have revealed conflicting conclusions about the direct effects of vibration on cancer cell invasion. Specifically, in breast cancer, Yi et al. (2020) previously demonstrated that 20-minute bouts of low intensity vibration (0.3 g, 90 Hz) applied directly twice daily for three days suppressed invasion of MDA-MB 231 cells.[24] However, Olcum et al. (2014) discovered that vibration (0.15 g and 90 Hz for 15 minutes/day, 5 days per week for 19 days) had no effects on MDA-MB 231 cell migration.[25] While the differences in the effects may be due to differences in the magnitudes, frequencies or duration of vibration, differences in the assays preformed may also impact results. Namely, Olcum et al. (2014) used a scratch assay where MDA-MB 231 cells were grown to confluency and the gap between cells following the creation of a scratch was calculated over 24 h. Additionally, Yi et al. (2020) performed an invasion assay with Matrigel to assess breast cancer cell invasion. The inclusion of Matrigel provides a barrier through which the breast cancer cells penetrate which closely mimic aspects of tissue invasion. In contrast, our bone metastasis-on-a-chip platform integrates both endothelial cells and a hydrogel matrix. The inclusion of the relevant cells and the hydrogel matrix serves as a more complex and physiologically relevant extracellular matrix compared to the use of the Matrigel alone. These differences emphasize the use of more physiologically relevant models, such as our bone metastasis-on-a-chip platform, to incorporate multiple cell types and ECM components that can provide valuable insights into the complex processes underlying cancer metastasis.

To discover potential mechanisms involved in this process, we explored the impact of vibration-stimulated osteocytes on prostate cancer cell adhesion to endothelial cells, mimicking the extravasation process. Our results revealed a significant decrease in the adhesion of PC3 cells to endothelial monolayer treated with conditioned media from vibration-stimulated osteocytes. This suggests that LMHF vibration may modulate osteocyte-secreted factors that influence the adhesive properties of endothelial cells, potentially impeding the ability of prostate cancer cells to extravasate into the bone. Notably, previous work by Chen et al. (2015) indicated that VCAM-1 expression on endothelial cells serves as a critical mediator for the adhesion of PC3s onto HUVECs which leads to subsequent metastasis into secondary sites.[60] That is, inflammatory cytokines induce the expression of VCAM-1 on the endothelium to promote the capture and adhesion of circulating tumor cells through binding with CD-44 on prostate cancer cells. By reducing VCAM-1 expression, less cancer cells adhere onto the endothelium and extravasate between the endothelial cells of the vessel well.[60]

By blocking VCAM-1 in both experimental groups in our study, as well as quantifying VCAM-1 expression by measuring fluorescence intensity, it allowed us to determine whether the expression of VCAM-1 was being altered and was responsible for the difference in adhesion following treatment with CM from static or vibration-stimulated osteocytes (Fig. 8). Our data demonstrated that VCAM-1 was indeed reduced and was likely responsible for the reduction in both extravasation distance and the number of extravasated cells.

Most importantly, the results also suggest that vibration-stimulated osteocytes may act in a similar manner to fluid flow-stimulated osteocytes activated by physical exercise. Work by Ma et al. (2019) determined similar effects on breast cancer cells and osteocytes stimulated with oscillatory fluid flow to examine the effects of physical exercise on breast cancer metastasis *in vitro*.[58] It was also discovered that by blocking intercellular adhesion molecule 1 (ICAM-1) on endothelial cells, the pattern in reduction of breast cancer cells adhering to the endothelial cells was no longer observed. This provides evidence suggesting that based on *in vitro* experiments, LMHF vibration may stimulate osteocytes in a similar way as physical exercise.

While our study does not examine the soluble factors secreted by vibration-stimulated osteocytes, various molecules and cytokines are implicated in the regulation of adhesion molecules on endothelial cells. For example, exogenous PGE2 and IL-8 has been shown to increase VCAM-1 expression on human umbilical vein endothelial cells.[61] Our lab has previously demonstrated that osteocytes treated with LMHF vibration have significantly lower levels of PGE2 expression.[36] Taken together, this may indicate that the reduced expression and secretion of PGE2 in vibration-stimulated osteocytes may be responsible for the decrease in expression of VCAM-1 and the subsequent adhesion of prostate cancer cells. However, further molecular analyses are required to determine the precise soluble factors secreted by osteocytes and their effects on endothelial cells.

Nevertheless, our data suggests that mechanically stimulated osteocytes can reduce extravasation by indirectly altering the adhesion of endothelial cells. These findings also collectively support our hypothesis that vibration-stimulated osteocytes can attenuate prostate cancer cell extravasation, providing novel insights into the potential therapeutic applications of LMHF vibration in the context of prostate cancer bone metastasis.

Moreover, several other mechanisms have been suggested regarding the role of mechanically loaded osteocytes in the regulation of cancer bone metastasis. Namely, osteocytes experiencing mechanical loading can regulate osteoblast activity through the downregulation of sclerostin, and increased release of prostaglandin E2 and nitric oxide, which work to enhance osteoblast activity through increased osteoblast proliferation and differentiation.[62–64] Coupling previous findings that demonstrate an increase in osteoblast activity which may offset the effects of tumor-induced osteolysis with our current data that suggests that LMHF vibration decreases PC3 extravasation, this suggests that LMHF vibration may be effective at reducing the incidence of bone metastases and its negative effects. Moreover, it's a well-established fact that the sinusoidal blood vessels of the bone marrow are leakier to allow for increased movement of hematopoietic cells.[65] That very leakiness also allows for cancer cells to extravasate. Additionally, the blood flow is also slower in these areas meaning cancer cells can interact with the endothelial cells for a greater period of time.[66] It has been previously shown that mechanically loaded osteocytes can secrete factors that reduce the permeability of HUVECs.[58] Specifically, the CM extracted from mechanically loaded MLO-Y4 cells resulted in endothelial cells that were 15% less permeable. However, future experiments examining how LMHF vibration stimulated CM alters endothelial cell permeability can be carried out to further demonstrate the benefits of LMHF vibration.

In sum, the findings of this paper can largely be divided into two main parts – the effects of the direct application of LMHF vibration on prostate cancer cells and the effects of LMHF vibration-stimulated osteocytes on prostate cancer cell extravasation. The distinction is critical for the clinical applications of these findings. Specifically, while whole body vibration may be used stimulate bones in the body, local vibration therapy may also be used to decrease the clonogenic and proliferative potential of prostate cancer cells for more targeted effects within the primary tumor site. As such, the translational prospects of LMHF vibration therapy offer a novel avenue for enhancing the efficacy of prostate cancer treatment to improve patient outcomes in the clinical setting. Nonetheless, while our findings suggest a significant decrease in prostate cancer cell growth and colony formation, our results do not demonstrate a complete eradication of prostate cancer nor a complete inhibition of prostate cancer extravasation. Rather, the results support that LMHF vibration has the potential to reduce tumorigenic properties of PCa either directly or through the stimulation of osteocytes. Additional experiments are required to fully investigate how

LMHF vibration could be employed in conjunction with existing therapies to further enhance the beneficial effects.

Nevertheless, while the work presented in this study offers novel insights into the effects of LMHF vibration on PC3 growth and bone metastasis, the experiments conducted are not without their limitations. Firstly, given that all the experiments carried out in this study were performed using *in vitro* models, vibration treatment was directly administered onto the cells. However, some concerns regarding the transmissibility of vibration in the clinical setting have been raised by other researchers. Specifically, the benefits of whole-body vibration therapy and its transmissibility has been shown to be dependent on several factors including a participant's posture, nonlinearities in the human musculoskeletal system, age differences, sex differences and the characteristics of the bone and bone marrow (trabecular versus cortical).[67] The vibration signal must travel through multiple tissue layers and the magnitude and frequency of the signal may be attenuated by the body's complex biomechanical properties. All our experiments were carried out by directly placing cells on the vibration platform with near perfect transmissibility. Thus, while the *in vitro* findings presented in this work are promising, translating these parameters for clinical or *in vivo* studies may require consideration for additional variables to ensure similar outcomes.

Secondly, we examined the effects of LMHF vibration on key tumorigenic properties such as cell growth, proliferation, colony formation and cell death. Further work examining oncogenic characteristics such as the expression of known oncogenes, tumor suppressor genes or properties such as dormancy or cellular senescence would provide greater evidence regarding the beneficial effects of vibration. Likewise, in some images, the static spheroids appear to have a less optically dense perimeter at days 3 and 4. Future studies are needed to determine whether this effect is due to LMHF vibration rearranging the cells or if the cells in the static spheroids exhibit greater proliferation in the outer layer.

Lastly, we employed a bone metastasis-on-a-chip device to examine how vibration-stimulated osteocytes impact PC3 extravasation. While the device allows us to explore several properties such as cellular crosstalk, invasion and extravasation all while incorporating mechanical stimuli into the microenvironment, previous limitations have been highlighted in the work done by Mei et al. (2019).[37] Specifically, the osteocyte channel does not recapitulate the complex lacunar-canalicular system of the bone but rather employs a simplistic collagen coated channel. Furthermore, the concentration of PC3 cells seeded into the lumen is much higher than the amount of circulating tumor cells found within the bloodstream of a patient with stage IV PCa.[68] While the total number may not be physiologically relevant, the microfluidic device was employed to investigate the role of MLO-Y4s in regulating PC3 bone extravasation. Lastly, the device combines both mouse (MLO-Y4) and human cell lines (HUVEC, PC3). The use of such established cell lines poses concerns about interspecies variation but also allows for the cells to be compared with existing literature due to their widely used nature. While certain features of the device may be improved in future studies, the findings from the bone metastasis-on-a-chip platform may serve as a valuable starting point to understand the interplay between mechanical cues and cancer cell behaviour in bone metastasis.

5. Conclusion

This study demonstrates that daily application of LMHF vibration negatively affects the proliferative capacity of prostate cancer cells *in vitro*. Specifically, the decrease in both the total number and percent area of colonies, along with the reduction in spheroid diameter, suggests that LMHF vibration may influence the proliferative capacity and clonogenic potential of prostate cancer cells. This finding raises the possibility that LMHF vibration could be explored as an adjuvant therapy to limit the expansion of prostate cancer cell populations. Additionally, vibration stimulated osteocytes reduce prostate cancer extravasation into the bone through a decrease in prostate cancer adhesion to endothelial cells, a key process that commences cancer colonization within the bone. Nevertheless, further investigation is required to unravel molecular mechanisms underlying the effects of vibration on prostate cancer cells and the bone microenvironment. Additionally, future studies should concentrate on investigating the potential synergistic effects of LMHF vibration with existing cancer therapies such as chemotherapy, radiation, and immunotherapy to enhance treatment efficacy. Nevertheless, these findings lay foundational groundwork for the clinical exploration of mechanical interventions in cancer treatment.

Funding support

This study was supported by the Natural Science and Engineering Research Council (NSERC, Grant No: 06465-14).

Ethical approval

This study does not contain any studies with human or animal subjects performed by any of the authors.

CRediT authorship contribution statement

Amel Sassi: Writing – review & editing, Writing – original draft, Methodology, Formal analysis, Data curation. **Kimberly Seaman:** Methodology, Data curation. **Xin Song:** Methodology, Data curation. **Chun-Yu Lin:** Methodology. **Yu Sun:** Writing – review & editing. **Lidan You:** Writing – review & editing, Supervision, Conceptualization.

Declaration of competing interest

The authors declare that they have no known competing financial interests or personal relationships that could have appeared to influence the work reported in this paper.

Appendix A. Supplementary data

Supplementary data to this article can be found online at https://doi.org/10.1016/j.mbm.2024.100095.

References

1. Morrissey C, Vessella RL. The role of tumor microenvironment in prostate cancer bone metastasis. *J Cell Biochem*. 2007;101:873–886. https://doi.org/10.1002/jcb.21214.
2. Siegel RL, Miller KD, Wagle NS, Jemal A. Cancer statistics, 2023. CA A. *Cancer J Clinicians*. 2023;73:17–48. https://doi.org/10.3322/caac.21763.
3. Thobe MN, Clark RJ, Bainer RO, Prasad SM, Rinker-Schaeffer CW. From prostate to bone: key players in prostate cancer bone metastasis. *Cancers*. 2011;3:478–493. https://doi.org/10.3390/cancers3010478.
4. Benke IN, Leitzmann MF, Behrens G, Schmid D. Physical activity in relation to risk of prostate cancer: a systematic review and meta-analysis. *Annals of Oncology, 3 or 6 months adjuvant chemotherapy for patients with stage III colon cancer?* 2018;29:1154–1179. https://doi.org/10.1093/annonc/mdy073.
5. Misiąg W, Piszczyk A, Szymańska-Chabowska A, Chabowski M. Physical activity and cancer care—a review. *Cancers (Basel)*. 2022;14:4154. https://doi.org/10.3390/cancers14174154.
6. Inoue M, JPHC Study Group. Impact of lifestyle on overall cancer risk among Japanese: the Japan public health center-based prospective study (JPHC study). *J Epidemiol*. 2010;20:90–96. https://doi.org/10.2188/jea.je20090209.
7. Lee C-D, Sui X, Hooker SP, Hébert JR, Blair SN. Combined impact of lifestyle factors on cancer mortality in men. *Ann Epidemiol*. 2011;21:749–754. https://doi.org/10.1016/j.annepidem.2011.04.010.
8. Westerlind KC. Physical activity and cancer prevention–mechanisms. *Med Sci Sports Exerc*. 2003;35:1834–1840. https://doi.org/10.1249/01.MSS.0000093619.37805.B7.
9. Kim J-S, Galvão DA, Newton RU, Gray E, Taaffe DR. Exercise-induced myokines and their effect on prostate cancer. *Nat Rev Urol*. 2021;18:519–542. https://doi.org/10.1038/s41585-021-00476-y.
10. Ballard-Barbash R, Friedenreich CM, Courneya KS, Siddiqi SM, McTiernan A, Alfano CM. Physical activity, biomarkers, and disease outcomes in cancer survivors: a systematic review. *J Natl Cancer Inst*. 2012;104:815–840. https://doi.org/10.1093/jnci/djs207.

11. Fong DYT, Ho JWC, Hui BPH, et al. Physical activity for cancer survivors: meta-analysis of randomised controlled trials. *BMJ*. 2012;344:e70. https://doi.org/10.1136/bmj.e70.
12. Riehl BD, Kim E, Bouzid T, Lim JY. The role of microenvironmental cues and mechanical loading milieus in breast cancer cell progression and metastasis. *Front Bioeng Biotechnol*. 2021;8.
13. Onal S, Alkaisi MM, Nock V. Application of sequential cyclic compression on cancer cells in a flexible microdevice. *PLOS ONE*. 2023;18:e0279896. https://doi.org/10.1371/journal.pone.0279896.
14. Baratchi S, Khoshmanesh K, Woodman OL, Potocnik S, Peter K, McIntyre P. Molecular sensors of blood flow in endothelial cells. *Trends Mol Med*. 2017;23:850–868. https://doi.org/10.1016/j.molmed.2017.07.007.
15. Hajra L, Evans AI, Chen M, Hyduk SJ, Collins T, Cybulsky MI. The NF-kappa B signal transduction pathway in aortic endothelial cells is primed for activation in regions predisposed to atherosclerotic lesion formation. *Proc Natl Acad Sci U S A*. 2000;97:9052–9057. https://doi.org/10.1073/pnas.97.16.9052.
16. Beck FX, Burger-Kentischer A, Müller E. Cellular response to osmotic stress in the renal medulla. *Pflugers Arch*. 1998;436:814–827. https://doi.org/10.1007/s004240050710.
17. Henke E, Nandigama R, Ergün S. Extracellular matrix in the tumor microenvironment and its impact on cancer therapy. *Front Mol Biosci*. 2020;6:160. https://doi.org/10.3389/fmolb.2019.00160.
18. Runel G, Lopez-Ramirez N, Chlasta J, Masse I. Biomechanical properties of cancer cells. *Cells*. 2021;10:887. https://doi.org/10.3390/cells10040887.
19. Ansaryan S, Khayamian MA, Saghafi M, et al. Stretch induces invasive phenotypes in breast cells due to activation of aerobic-glycolysis-related pathways. *Adv Biosyst*. 2019;3:e1800294. https://doi.org/10.1002/adbi.201800294.
20. Wang Y, Goliwas KF, Severino PE, et al. Mechanical strain induces phenotypic changes in breast cancer cells and promotes immunosuppression in the tumor microenvironment. *Lab Invest*. 2020;100:1503–1516. https://doi.org/10.1038/s41374-020-0452-1.
21. Riehl BD, Kim E, Lee JS, et al. The role of fluid shear and metastatic potential in breast cancer cell migration. *J Biomech Eng*. 2020;142:101001. https://doi.org/10.1115/1.4047076.
22. Choi HY, Yang G-M, Dayem AA, et al. Hydrodynamic shear stress promotes epithelial-mesenchymal transition by downregulating ERK and GSK3β activities. *Breast Cancer Res*. 2019;21:6. https://doi.org/10.1186/s13058-018-1071-2.
23. Zhang X, Yang L, Chien S, Lv Y. Suspension state promotes metastasis of breast cancer cells by up-regulating cyclooxygenase-2. *Theranostics*. 2018;8:3722–3736. https://doi.org/10.7150/thno.25434.
24. Yi X, Wright LE, Pagnotti GM, et al. Mechanical suppression of breast cancer cell invasion and paracrine signaling to osteoclasts requires nucleo-cytoskeletal connectivity. *Bone Res*. 2020;8:1–13. https://doi.org/10.1038/s41413-020-00111-3.
25. Olcum M, Ozcivici E. Daily application of low magnitude mechanical stimulus inhibits the growth of MDA-MB-231 breast cancer cells in vitro. *Cancer Cell Int*. 2014;14:102. https://doi.org/10.1186/s12935-014-0102-z.
26. Xiong X, Huo Q, Li K, et al. Enhancing anti-tumor potential: low-intensity vibration suppresses osteosarcoma progression and augments MSCs' tumor-suppressive abilities. *Theranostics*. 2024;14:1430–1449. https://doi.org/10.7150/thno.90945.
27. Liu X, Yu J, Song S, Yue X, Li Q. Protease-activated receptor-1 (PAR-1): a promising molecular target for cancer. *Oncotarget*. 2017;8:107334–107345. https://doi.org/10.18632/oncotarget.21015.
28. Zigler M, Kamiya T, Brantley EC, Villares GJ, Bar-Eli M. PAR-1 and thrombin: the ties that bind the microenvironment to melanoma metastasis. *Cancer Res*. 2011;71:6561–6566. https://doi.org/10.1158/0008-5472.CAN-11-1432.
29. Keller ET. The role of osteoclastic activity in prostate cancer skeletal metastases. *Drugs Today (Barc)*. 2002;38:91–102. https://doi.org/10.1358/dot.2002.38.2.820105.
30. Sottnik JL, Keller ET. Understanding and targeting osteoclastic activity in prostate cancer bone metastases. *Curr Mol Med*. 2013;13:626–639.
31. Lipton A, Uzzo R, Amato RJ, et al. The science and practice of bone health in oncology: managing bone loss and metastasis in patients with solid tumors. *J Natl Compr Cancer Netw*. 2009;7:S1–S30.
32. Coleman RE. Metastatic bone disease: clinical features, pathophysiology and treatment strategies. *Cancer Treat Rev*. 2001;27:165–176. https://doi.org/10.1053/ctrv.2000.0210.
33. Klein-Nulend J, Bacabac RG, Bakker AD. Mechanical loading and how it affects bone cells: the role of the osteocyte cytoskeleton in maintaining our skeleton. *Eur Cell Mater*. 2012;24:278–291. https://doi.org/10.22203/ecm.v024a20.
34. Song X, Lin C-Y, Mei X, Wang L, You L. Reduction of breast cancer extravasation via vibration activated osteocyte regulation. *iScience*. 2022;25:105500. https://doi.org/10.1016/j.isci.2022.105500.
35. Lin C-Y, Song X, Ke Y, et al. Yoda 1 enhanced low-magnitude high-frequency vibration on osteocytes in regulation of MDA-MB-231 breast cancer cell migration. *Cancers (Basel)*. 2022;14:3395. https://doi.org/10.3390/cancers14143395.
36. Lau E, Al-Dujaili S, Guenther A, Liu D, Wang L, You L. Effect of low-magnitude, high-frequency vibration on osteocytes in the regulation of osteoclasts. *Bone*. 2010;46:1508–1515. https://doi.org/10.1016/j.bone.2010.02.031.
37. Mei X, Middleton K, Shim D, et al. Microfluidic platform for studying osteocyte mechanoregulation of breast cancer bone metastasis. *Integr Biol*. 2019;11:119–129. https://doi.org/10.1093/intbio/zyz008.
38. Rahn JJ, Chow JW, Horne GJ, et al. MUC1 mediates transendothelial migration in vitro by ligating endothelial cell ICAM-1. *Clin Exp Metastasis*. 2005;22:475–483. https://doi.org/10.1007/s10585-005-3098-x.
39. Oschwald V, Prokop A, Maas V, et al. Whole-body vibration training for inpatient children and adolescents receiving chemotherapy for first cancer diagnosis: an exploratory feasibility study. *Ger J Exerc Sport Res*. 2023;53:30–36. https://doi.org/10.1007/s12662-022-00820-3.
40. Baker MK, Peddle-McIntyre CJ, Galvão DA, Hunt C, Spry N, Newton RU. Whole body vibration exposure on markers of bone turnover, body composition, and physical functioning in breast cancer patients receiving aromatase inhibitor therapy: a randomized controlled trial. *Integr Cancer Ther*. 2018;17:968–978. https://doi.org/10.1177/1534735418781489.
41. Seefried L, Genest F, Strömsdörfer J, et al. Impact of whole-body vibration exercise on physical performance and bone turnover in patients with monoclonal gammopathy of undetermined significance. *J Bone Oncol*. 2020;25:100323. https://doi.org/10.1016/j.jbo.2020.100323.
42. de Sire A, Lippi L, Ammendolia A, et al. Physical exercise with or without whole-body vibration in breast cancer patients suffering from aromatase inhibitor—induced musculoskeletal symptoms: a pilot randomized clinical study. *J Personalized Med*. 2021;11:1369. https://doi.org/10.3390/jpm11121369.
43. Vontela N, Kovesdy C, Latif Z, Lane R, Weir A. Prevalence and incidence of immune thrombocytopenia in patients with prostate cancer. *Am J Med Sci*. 2018;356:499–500. https://doi.org/10.1016/j.amjms.2018.05.003.
44. Betsch DM, Gray S, Zed SE. A case of metastatic prostate cancer and immune thrombocytopenia. *Curr Oncol*. 2017;24:434–436. https://doi.org/10.3747/co.24.3592.
45. Sriuranpong V, Borges MW, Ravi RK, et al. Notch signaling induces cell cycle arrest in small cell lung cancer Cells1. *Cancer Res*. 2001;61:3200–3205.
46. Enderle-Ammour K, Bader M, Ahrens TD, et al. Form follows function: morphological and immunohistological insights into epithelial–mesenchymal transition characteristics of tumor buds. *Tumour Biol*. 2017;39:1010428317705501. https://doi.org/10.1177/1010428317705501.
47. Pagnotti GM, Chan ME, Adler BJ, et al. Low intensity vibration mitigates tumor progression and protect bone quantity and quality in a murine model of myeloma. *Bone*. 2016;90:69–79. https://doi.org/10.1016/j.bone.2016.05.014.
48. Pagnotti GM, Adler BJ, Green DE, et al. Low magnitude mechanical signals mitigate osteopenia without compromising longevity in an aged murine model of spontaneous granulosa cell ovarian cancer. *Bone*. 2012;51:570–577. https://doi.org/10.1016/j.bone.2012.05.004.
49. Abidine Y, Constantinescu A, Laurent VM, et al. Mechanosensitivity of cancer cells in contact with soft substrates using AFM. *Biophys J*. 2018;114:1165–1175. https://doi.org/10.1016/j.bpj.2018.01.005.
50. Rianna C, Radmacher M, Kumar S. Direct evidence that tumor cells soften when navigating confined spaces. *Mol Biol Cell*. 2020;31:1726–1734. https://doi.org/10.1091/mbc.E19-10-0588.
51. Heyden S, Ortiz M. Oncotripsy: targeting cancer cells selectively via resonant harmonic excitation. *J Mech Phys Solid*. 2016;92:164–175. https://doi.org/10.1016/j.jmps.2016.04.016.
52. Zimmerman JW, Jimenez H, Pennison MJ, et al. Targeted treatment of cancer with radiofrequency electromagnetic fields amplitude-modulated at tumor-specific frequencies. *Chin J Cancer*. 2013;32:573–581. https://doi.org/10.5732/cjc.013.10177.
53. You L, Temiyasathit S, Lee P, et al. Osteocytes as mechanosensors in the inhibition of bone resorption due to mechanical loading. *Bone*. 2008;42:172–179. https://doi.org/10.1016/j.bone.2007.09.047.
54. Fan Y, Jalali A, Chen A, et al. Skeletal loading regulates breast cancer-associated osteolysis in a loading intensity-dependent fashion. *Bone Res*. 2020;8:1–11. https://doi.org/10.1038/s41413-020-0083-6.
55. van Santen VJB, Jin J, Hogervorst JMA, Bakker AD. Shear loaded osteocyte-like-cells affect epithelial and mesenchymal gene expression in DU145 prostate cancer cells, while decreasing their invasion in vitro. *Biochem Biophys Res Commun*. 2023;646:70–77. https://doi.org/10.1016/j.bbrc.2023.01.066.
56. Li F, Chen A, Reeser A, et al. Vinculin force sensor detects tumor-osteocyte interactions. *Sci Rep*. 2019;9:5615. https://doi.org/10.1038/s41598-019-42132-x.
57. Dwivedi A, Kiely PA, Hoey DA. Mechanically stimulated osteocytes promote the proliferation and migration of breast cancer cells via a potential CXCL1/2 mechanism. *Biochem Biophys Res Commun*. 2021;534:14–20. https://doi.org/10.1016/j.bbrc.2020.12.016.
58. Ma Y-HV, Xu L, Mei X, Middleton K, You L. Mechanically stimulated osteocytes reduce the bone-metastatic potential of breast cancer cells in vitro by signaling through endothelial cells. *J Cell Biochem*. 2019;120:7590–7601. https://doi.org/10.1002/jcb.28034.
59. Verbruggen SW, Thompson CL, Duffy MP, et al. Mechanical stimulation modulates osteocyte regulation of cancer cell phenotype. *Cancers (Basel)*. 2021;13:2906. https://doi.org/10.3390/cancers13122906.
60. Chen C, Zhang Q, Liu S, et al. IL-17 and insulin/IGF1 enhance adhesion of prostate cancer cells to vascular endothelial cells through CD44-VCAM-1 interaction. *Prostate*. 2015;75:883–895. https://doi.org/10.1002/pros.22971.
61. Winkler M, Kemp B, Hauptmann S, Rath W. Parturition: steroids, prostaglandin E2, and expression of adhesion molecules by endothelial cells. *Obstetrics Gynecol*. 1997;89:398–402. https://doi.org/10.1016/S0029-7844(96)00500-5.
62. Robling AG, Niziolek PJ, Baldridge LA, et al. Mechanical stimulation of bone in vivo reduces osteocyte expression of Sost/sclerostin. *J Biol Chem*. 2008;283:5866–5875. https://doi.org/10.1074/jbc.M705092200.
63. Fox SW, Chambers TJ, Chow JW. Nitric oxide is an early mediator of the increase in bone formation by mechanical stimulation. *Am J Physiol*. 1996;270:E955–E960. https://doi.org/10.1152/ajpendo.1996.270.6.E955.

64. Li L, Yang Z, Zhang H, Chen W, Chen M, Zhu Z. Low-intensity pulsed ultrasound regulates proliferation and differentiation of osteoblasts through osteocytes. *Biochem Biophys Res Commun*. 2012;418:296–300. https://doi.org/10.1016/j.bbrc.2012.01.014.
65. Itkin T, Gur-Cohen S, Spencer JA, et al. Distinct bone marrow blood vessels differentially regulate haematopoiesis. *Nature*. 2016;532:323–328. https://doi.org/10.1038/nature17624.
66. Mazo IB, von Andrian UH. Adhesion and homing of blood-borne cells in bone marrow microvessels. *J Leukoc Biol*. 1999;66:25–32. https://doi.org/10.1002/jlb.66.1.25.
67. Song X, Sassi A, Seaman K, Lin C-Y, You L. Vibration therapy for cancer-related bone diseases. *Vibrations*. 2023;6:449–465. https://doi.org/10.3390/vibration6020028.
68. Cieślikowski WA, Antczak A, Nowicki M, Zabel M, Budna-Tukan J. Clinical relevance of circulating tumor cells in prostate cancer management. *Biomedicines*. 2021;9:1179. https://doi.org/10.3390/biomedicines9091179.